

FUNCTION

## Three-Directional Myocardial Motion Assessed Using 3D Phase Contrast MRI

John-Peder Escobar Kvitting,<sup>1,2,\*</sup> Tino Ebbers,<sup>1,2</sup> Jan Engvall,<sup>1,2</sup>  
George R. Sutherland,<sup>3</sup> Bengt Wranne,<sup>1,2</sup> and Lars Wigström<sup>1,2</sup>

<sup>1</sup>Department of Clinical Physiology and <sup>2</sup>Center for Medical Image Science  
and Visualization, Linköping University, Linköping, Sweden

<sup>3</sup>Department of Cardiology, University Hospital Gasthuisberg, Leuven, Belgium

### ABSTRACT

Regional myocardial function is a complex entity consisting of motion in three dimensions (3D). Besides magnetic resonance imaging (MRI), no other noninvasive technique can give a true 3D description of cardiac motion. Using a time-resolved 3D phase contrast technique, three-dimensional image volumes containing myocardial velocity data in six normal volunteers were acquired. Coordinates and velocity information were extracted from nine points placed in different myocardial segments in the left ventricle (LV), and decomposed into longitudinal ( $V_L$ ), radial ( $V_R$ ), and circumferential ( $V_C$ ) velocity components. Our findings confirm a longitudinal apex-to-base gradient for the LV, with only a small motion of the apex. The mean velocity for  $V_L$  for all the basal segments was higher compared to the midsegments during systole [ $3.5 \pm 1.2$  vs.  $2.5 \pm 1.7$  cm/s ( $p < 0.01$ )], early filling [ $-6.9 \pm 1.8$  vs.  $-4.9 \pm 1.8$  cm/s ( $p < 0.001$ )], and during atrial contraction [ $-2.2 \pm 1.4$  vs.  $-1.6 \pm 1.3$  cm/s ( $p < 0.05$ )]. A similar pattern was observed when comparing velocities from the midsegments to the apex. Radial velocity was higher during early filling in the midportion of the lateral [ $-4.9 \pm 2.7$  vs.  $-3.2 \pm 1.6$  cm/s ( $p < 0.05$ )] wall compared to the basal segments, no difference was observed for the septal [ $-2.0 \pm 1.5$  vs.  $-0.3 \pm 2.5$  cm/s ( $p = 0.15$ )], anterior [ $-5.8 \pm 3.3$  vs.  $-4.0 \pm 1.7$  cm/s ( $p = 0.17$ )], and posterior [ $-2.3 \pm 2.1$  vs.  $-2.5 \pm 1.0$  cm/s ( $p = 0.78$ )] walls. When observing the myocardial velocity in a single point and visualizing the movement of the main direction of the velocities in this point as vectors in velocity vector plots like planes, it is clear that

\*Correspondence: John-Peder Escobar Kvitting, M.D., Ph.D., Department of Clinical Physiology, Linköping University, Linköping, SE-581 85, Sweden; Fax: +46-13-145949; E-mail: johkv@imv.liu.se.

myocardial movement is by no means one dimensional. In conclusion, our time-resolved 3D, phase contrast MRI technique makes it feasible to extract myocardial velocities from anywhere in the myocardium, including all three velocity components without the need for positioning any slices at the time of acquisition.

*Key Words:* Myocardial velocities; Magnetic resonance imaging; Phase contrast; Three dimensional.

## INTRODUCTION

The left ventricle (LV) moves in a complex, three-dimensional (3D) pattern. The motion can, in every point, be divided into longitudinal (base to apex), radial (towards the centerline of the cavity), and circumferential (torsional) components. An adequate presentation of all three velocity components would enhance our understanding of the physiology and pathophysiology of regional myocardial function. Previously, the investigation of the heart in 3D has been limited to cineventriculography of implanted epicardial markers in animals and surgically treated patients, which does not allow the investigation of the untouched heart (Hansen et al., 1988; Ingels et al., 1989). Cardiac ultrasound using Doppler myocardial imaging (DMI) has made it possible to assess myocardial velocities and gradients in one direction noninvasively (Miyatake et al., 1995; Sutherland et al., 1994). Myocardial velocities acquired with DMI are, however, affected by the angle of insonation of the ultrasound beam from the transducer (Uematsu et al., 1995).

Magnetic resonance imaging (MRI) tagging with derived parameters such as strain can be performed by placing noninvasive tags that move and deform with the myocardium on which they are inscribed, and is not limited by the acoustic window of ultrasound (Axel and Dougherty, 1989; Bogaert and Rademakers, 2001; Zerhouni et al., 1988). Quantification of myocardial motion based on MRI tagging requires time-consuming postprocessing, which currently limits this method to research applications (Masood et al., 2000). Phase contrast MRI has proven to accurately describe motion in all three directions in a single point (Karwatowski et al., 1994; Pelc et al., 1994). Acquisition of velocities using MRI phase contrast will also make it possible to evaluate findings observed using DMI. A combination of multiple 2D slices acquired in different orientations can be used to produce a three-dimensional description of myocardial motion (Holman et al., 1997; Kayser et al., 2000). However, using a 2D MRI technique, the slices of interest have to be placed prior to the acquisition, and the slices will give a sparse representation of the heart. Information from an image volume

covering the entire heart will make it possible to define the region of interest anywhere after the acquisition of the data. A three-directional velocity data set will then make it possible to determine the main direction of the velocity vector along the three main axes of the left ventricle, and thereby improve our understanding of cardiac physiology. Also, it will enable us to assess the limitations of a 1D or 2D approach to regional myocardial function.

The aim of the present study is to describe a phase contrast MRI technique for acquiring velocity information that assesses the three-directional motion of the human heart.

## METHODS

### Study Population

Six normal volunteers (one female), mean age 40 years (range, 25–56 years) with a normal 12-lead electrocardiogram, without visible echocardiographic motion abnormalities, and no family history of cardiovascular disease were included in the study. All subjects were in sinus rhythm ( $65 \pm 8$ , bpm, range 52–73). The study was approved by the Regional Ethics Committee for Human Research at the Faculty of Health Sciences, Linköping University, and written informed consent was obtained from all the volunteers.

### Study Protocol

Velocity vector information was obtained using a time-resolved 3D phase contrast pulse sequence (Wigström et al., 1996). The sequence is retrospectively gated, and since we acquire data from a full 3D volume of interest, the velocity information can be studied anywhere within the myocardium, without the need to accurately position any slices at the time of data acquisition. A 1.5 T MRI scanner (Signa LX Echospeed, GE Medical Systems, Milwaukee, WI) and the following acquisition parameters were used: repetition time (TR)=27 ms, echo time (TE)=8 ms, velocity encoding (VENC)=18 cm/s, field-of-view



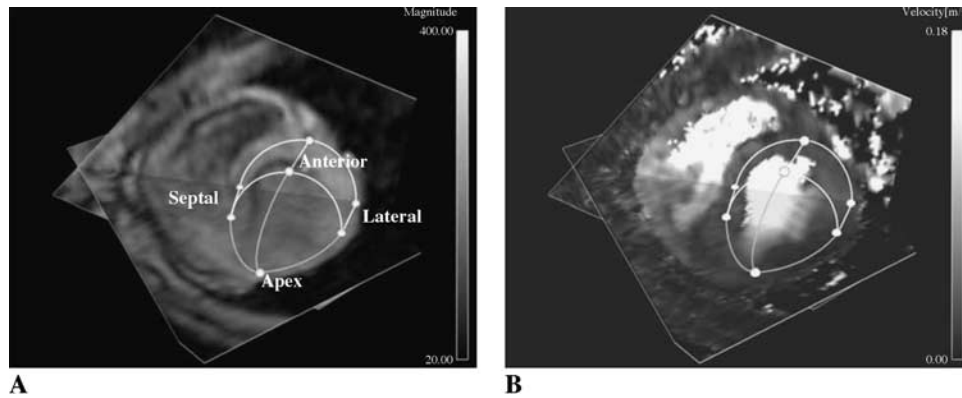


**Figure 1.** Phase contrast MRI images of two intersecting planes extracted from the 3D volume data in peak systole. Magnitude image (A) and the total velocity data (B) displayed with a schematic wire frame made from the points used in the velocity analysis.

(FOV)= $300 \times 300 \times 128$  mm with a spatial resolution of  $1 \times 4 \times 4$  mm, with an acquisition time of 32 minutes. Two of the data sets were acquired using the reduced field of view approach (Madore et al., 2000). To suppress artifacts from pulsatile blood flow, spatial saturation pulses were applied superiorly and inferiorly to the acquired volume (Drangova et al., 1997). The phase contribution from concomitant gradient (Maxwell) terms and eddy current effects was subtracted (Bernstein et al., 1998). The velocity data was transformed to the Ensign<sup>®</sup> visualization program (CEI Inc, Research Triangle Park, NC) for further analysis (Wigström et al., 1999).

In the visualization program, a four-chamber plane was retrospectively extracted giving good delineation of the left ventricle (Fig. 1). Subsequently, two short axis planes were placed perpendicularly to the four-chamber plane; one plane below the mitral annulus and the next at the midpapillary level halfway between the former and the apex. Nine points were manually deployed within the myocardium in the following locations: the basal part of the lateral, septal, anterior, and posterior walls, the midventricular level of the same four walls, and at the apex (Fig. 2).

For each point, the spatial coordinates and the velocity information in all three directions through the 32 time frames were exported to Matlab<sup>®</sup> (Mathworks Inc., Natick, MA). The orientation for the longitudinal velocity vector,  $V_L$ , was defined as perpendicular to the short-axis plane. The radial velocity vector,  $V_R$ , was defined as the direction between the point and the center of the grid made by the four points forming a plane. The circumferential velocity vector,  $V_C$ , was defined as perpendicular to the vector pair formed by  $V_L$  and  $V_R$  (Fig. 2). Motion towards the apex was defined as positive for longitudinal velocity. For radial

motion, positive values corresponded to motion towards the center of the LV cavity. Circumferential positive values indicate clockwise motion seen from the apex. This procedure gives information related to a fixed point in space (Eulerian coordinates), i.e., the myocardium moves through the point of observation during the heart cycle in the same way as in the Doppler myocardial imaging and conventional blood pool Doppler techniques (DeGroff, 2003).

The timing of the peak velocity data for the systolic contraction (S-wave), early filling of the LV (E-wave), and atrial contraction (A-wave) was defined in each individual data set. Timing of the velocities was defined from the velocity curve of the longitudinal velocity component of the left ventricle based on the mean value of all nine points. The same time frames for the S, E, and A waves were then used for all four walls, including the apex and all three velocity components.

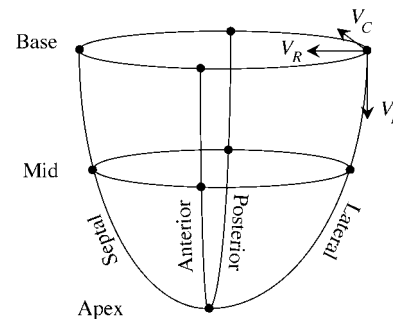


**Figure 2.** Schematic drawing demonstrating the two short-axis planes and the apical point forming the left ventricle. In every one of the nine points, three-directional velocity was extracted over time ( $V_L$ , longitudinal velocity component;  $V_R$ , radial velocity component; and  $V_C$ , circumferential velocity component).

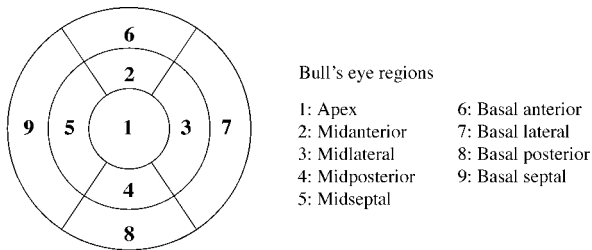


**Figure 3.** Bull's-eye diagram showing the defined regions of the left ventricle.

In order to show the direction of the motion of the myocardium during the cardiac cycle, velocity vector loops were created. This was performed by plotting the velocity vectors corresponding to a single point in the myocardium for every time frame over the cardiac cycle. By connecting the tips of the velocity vectors, loops were formed. In analogy with vectorcardiography, the vector information was displayed by projecting it onto three orthogonal planes (frontal, left sagittal, and horizontal). By combining the information from two of the three loops, information on the spatial

direction of the velocity was obtained. It is important to understand that the plots show the direction of the velocity vectors in space in one chosen point, and not the motion of the point.

All data are presented as mean±SD, and the values for the decomposed velocity components are presented in bull's-eye diagrams (Fig. 3). Student's *t*-test with dependent samples was used to analyze the difference between the myocardial segments. All calculations were performed with Statistica (StatSoft, Inc., Tulsa, OK). Statistical significance was set as  $p < 0.05$ .

### RESULTS

Data were extracted from the four walls of the left ventricle (LV), anterior, posterior, lateral, and septal. Waveforms corresponding to systolic contraction (S wave), early filling of the LV (E wave), and atrial contraction (A wave) were observed in all four walls (Fig. 4). The longitudinal ( $V_L$ ) component showed a clear velocity gradient from base to apex in all four walls, with highest velocities in the basal part (Fig. 5). The mean velocity for  $V_L$  for all basal segments was

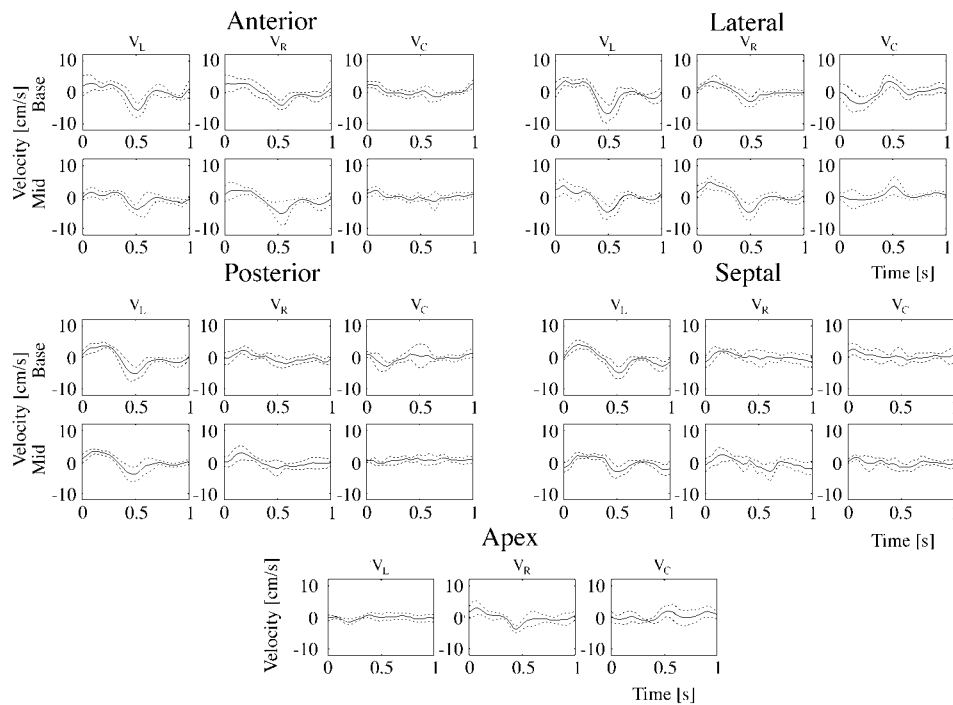


**Figure 4.** Velocity data (cm/s) from the anterior, posterior, septal, lateral wall, and the apex in six normal volunteers. First row of figures corresponds to the basal segments, second to middle segments for the four walls. Mean values (—)±standard deviation (---).  $V_L$  denotes longitudinal velocity component;  $V_R$ , radial velocity component; and  $V_C$ , circumferential velocity component.

Longitudinal

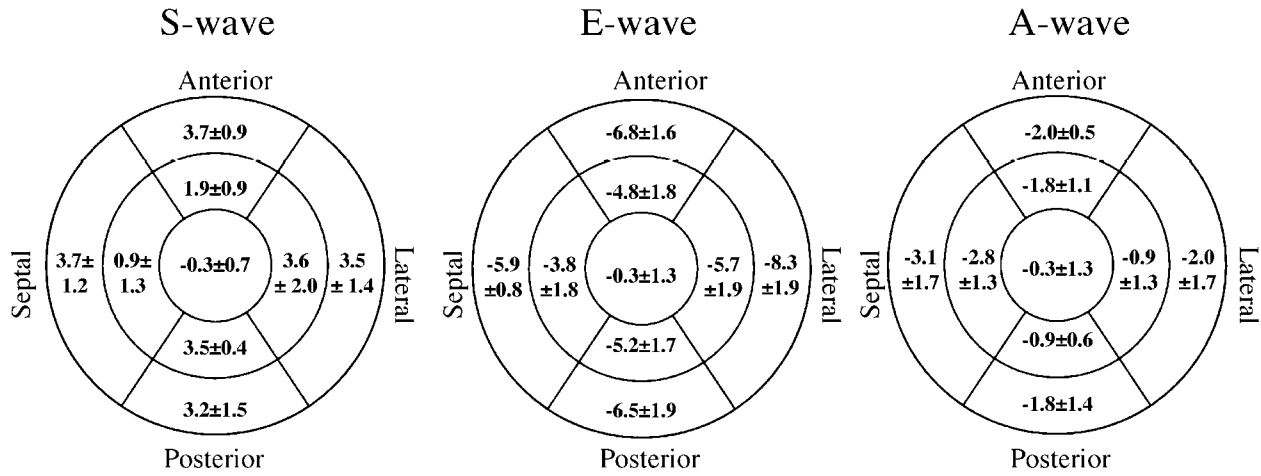


Figure 5. Longitudinal velocity component (cm/s). Mean values ± SD.

higher compared to the midsegments during the S wave [ $3.5 \pm 1.2$  vs.  $2.5 \pm 1.7$  cm/s ( $p < 0.01$ )], the E wave [ $-6.9 \pm 1.8$  vs.  $-4.9 \pm 1.8$  cm/s ( $p < 0.001$ )], and the A wave [ $-2.2 \pm 1.4$  vs.  $-1.6 \pm 1.3$  cm/s ( $p < 0.05$ )]. The same pattern was seen for the midsegments compared to the apical segment, higher velocity during systole [ $2.5 \pm 1.7$  vs.  $-0.3 \pm 0.7$  cm/s ( $p < 0.001$ )] and early filling [ $-4.9 \pm 1.8$  vs.  $-0.3 \pm 1.3$  cm/s ( $p < 0.001$ )], and during atrial contraction [ $-1.6 \pm 1.3$  vs.  $-0.3 \pm 1.3$  cm/s ( $p < 0.001$ )]. Apical movement in the longitudinal direction was almost zero.

The E-wave radial velocity ( $V_R$ ) was higher during early filling in the midportion of the lateral [ $-4.9 \pm 2.5$  vs.  $-3.2 \pm 1.6$  cm/s ( $p < 0.05$ )] walls compared to the basal segments, no difference was observed for the septal [ $-2.0 \pm 1.5$  vs.  $-0.3 \pm 2.5$  cm/s ( $p = 0.15$ )], anterior [ $-5.8 \pm 3.3$  vs.  $-4.0 \pm 1.7$  cm/s ( $p = 0.17$ )], and posterior [ $-2.3 \pm 2.1$  vs.  $-2.5 \pm 1.0$  cm/s ( $p = 0.78$ )] walls (Fig. 6). Finally, circumferential velocities (Fig. 7) were of the same magnitude as the longitudinal and radial ones, but there was no apparent base-to-apex gradient.

Radial

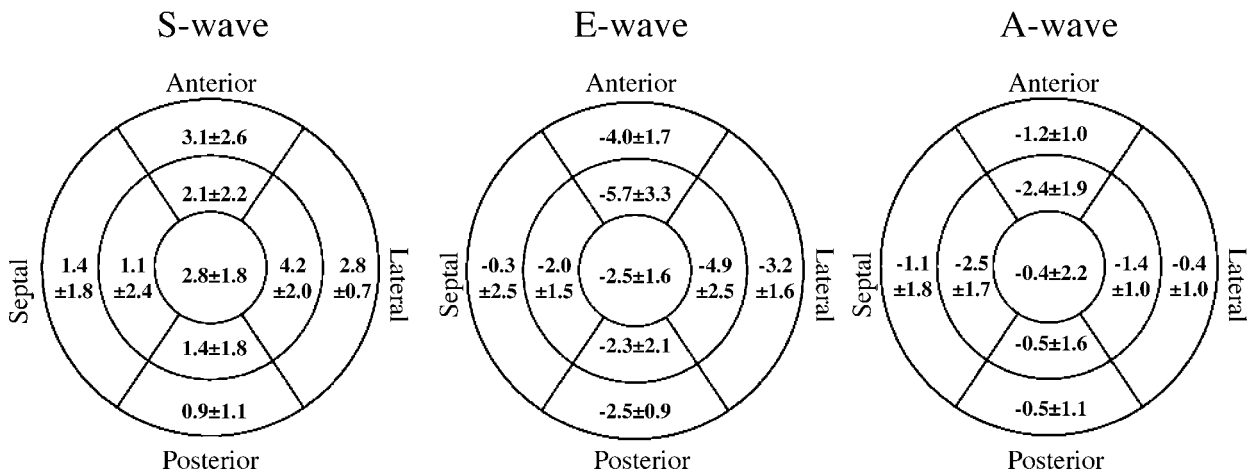


Figure 6. Radial velocity component (cm/s). Mean values ± SD.

### Circumferential

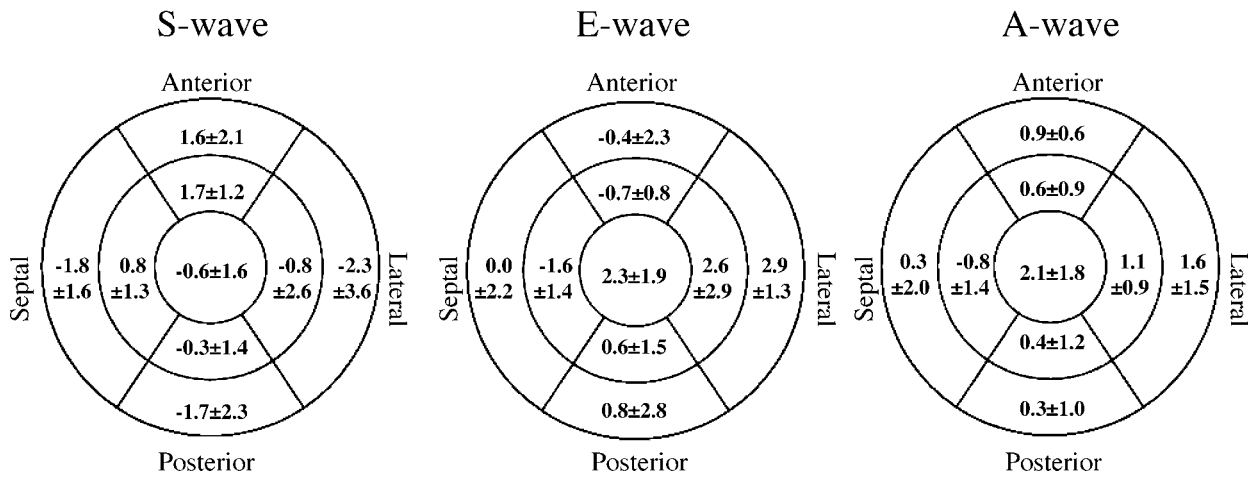


Figure 7. Circumferential velocity component (cm/s). Mean values±SD.

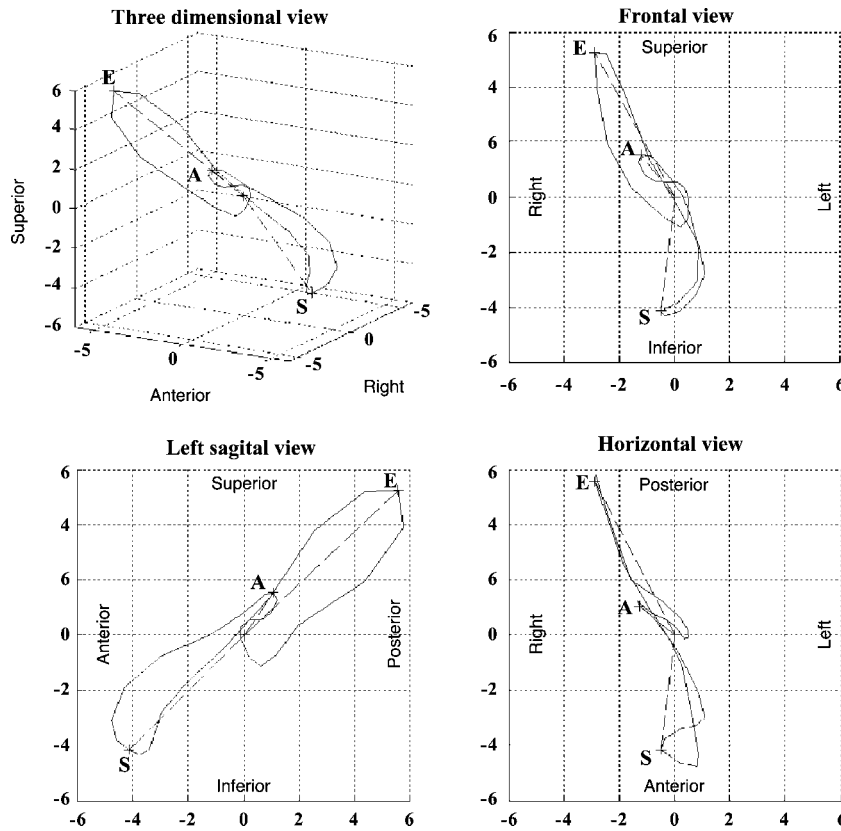


Figure 8. Velocity vector plots (cm/s) from a single point in the basal segment of the lateral wall of the left ventricle (average value from all the volunteers). S, systolic contraction; E, early diastolic filling; A, atrial contraction. Note that the plots show the direction of the velocity vectors in space in one chosen point, and not the motion of the point.

An interesting observation for the circumferential velocity ( $V_C$ ) is a clear pattern of motion in a clockwise manner (i.e., right-handed helix) during the E wave of the lateral wall. During the S wave, negative values are seen for the lateral and posterior, while the anterior and septal wall moves clockwise (positive values).

Points were extracted from LV, and one example from the basal part of the LV lateral wall is shown in Fig. 8. The direction of the velocities in this point over time is shown as a vector velocity loop. The direction of the main velocity vector from the point during the E wave and A wave are not parallel, but have different directions in 3D space. During systole the direction of the main velocity vector from the point is not  $180^\circ$  opposite to the direction during diastole. This pattern can be seen for all three projection planes.

## DISCUSSION

### Global vs. Regional Myocardial Function

Global parameters of cardiac function have a central role in the evaluation of cardiac disease. In coronary artery disease, global parameters such as ejection fraction (EF) may be normal. One possible reason for EF remaining within normal limits is that impaired function in one region of the ventricle is often accompanied by hyperkinesis elsewhere (Popp, 1990). It is therefore prudent to evaluate regional myocardial function, which is routinely done in both echocardiographic and angiographic investigations. However, regional motion of the heart, including flow as well as wall motion, is dynamic and three dimensional. Time-resolved 3D phase contrast MRI has previously been used to resolve flow velocities and local pressure variations (Wigström et al., 1999; Ebbers et al., 2002). The aim of this paper is to extend the technique to studies of regional myocardial function.

### Quantification of Regional Myocardial Function

Several new MRI techniques to estimate myocardial deformation have emerged over the last few years. Myocardial deformation can be intuitively seen in MRI tagging data, but quantitative strain analysis still requires advanced postprocessing techniques to automatically identify tag lines. Using harmonic imaging (HARP), the tagging data can be more rapidly analyzed

to give myocardial strain estimates (Osman et al., 1999; Ryf et al., 2002; Sampath et al., 2003), but the tagging data still suffer from a relatively low spatial resolution due to the required tag spacing and fading of the tag lines over the cardiac cycle. The use of tagging in combination with steady-state free precession (SSFP) acquisition techniques can result in an increased image contrast between blood and myocardium, or an improved tag persistence/contrast-to-noise ratio (Herzka et al., 2003; Zwanenburg et al., 2003). Displacement encoding with simulated echoes (DENSE) has been introduced as a new method to measure displacement to be used for strain estimation over a predetermined fraction of the cardiac cycle (Aletras et al., 1999). The DENSE method has also been shown to improve the image contrast separating myocardium from the blood pool (Aletras et al., 1999). Both the tagging/HARP and the DENSE approach will result in estimates of myocardial strain maps. Phase contrast (PC) MRI will instead provide velocity information that may be an important parameter to assess regional myocardial function as described in this paper, and can also be used in subsequent calculations of deformation parameters such as strain and strain rate.

Cardiac ultrasound using Doppler myocardial velocity imaging (DMI) has expanded as a technique to quantify regional myocardial function (Miyatake et al., 1995; Sutherland et al., 1994). Doppler myocardial imaging has made it possible to assess changes in velocity gradients across and along the walls, and has been suggested to be a possible indicator of myocardial contractility (Fleming et al., 1994; Gorcsan et al., 1996). However, DMI is limited to the in-plane movement and only measures one-velocity component (Miyatake et al., 1995).

Ingels and colleagues found the twist of the apex to be characteristic of left ventricular contraction (Ingels et al., 1989). It therefore seems important to include the apex in the assessment of regional myocardial function. With MRI, the movement of the apex can be analyzed in more detail in contrast to echocardiography, where the apical movement is lost in the near field of the transducer. Currently, only MRI, either as tagging or phase contrast, can noninvasively assess apical movement. The main problem with the apex is defining a proper coordinate system.

An important difference between our MRI technique and the epicardial marker studies in the assessment of regional myocardial function, is that the locations of the epicardial markers are tracked over time (Lagrangian coordinates), while our data is extracted from a fixed location in space (Eulerian coordinates)

(DeGroff, 2003). Similar Eulerian coordinate systems are used in DMI and pulsed Doppler imaging, making our findings of the movement of the heart more comparable to DMI (Hatle and Sutherland, 2000). The epicardial marker technique requires sternotomy and, usually, also cardiopulmonary bypass. This procedure in itself causes hypokinetic motion of the tricuspid annulus and paradoxical motion of the intraventricular septum (Wranne et al., 1991, 1993). Against this background it is difficult to translate findings from epicardial marker studies in animals or patients to results obtained from ultrasound or MRI.

### Myocardial Velocities

Time-resolved 3D phase contrast MRI provides data describing myocardial velocities in all parts of the left ventricle (LV) from a single acquisition. Our findings indicate a longitudinal apex-to-base gradient for all four walls of the LV, with limited movement of the apex. The velocity gradient was present during systole, early filling, and atrial contraction. The longitudinal gradient has been shown to be important for the function of LV filling and is affected early in left ventricular disease (Jones et al., 1990). In contrast to DMI, our data are not limited to one-directional velocity. Radial velocities are seen to be higher in the middle part of the lateral wall, but not for the septal, anterior and posterior part of the walls compared to the basal part of the LV. Our finding of higher values for the radial velocity components at midventricular level may be a result of the basal segments having their motion limited by the annulus fibrosus.

Using vector velocity plots to elucidate the movement of the ventricle, we have been able to describe the direction of the velocity vector from any point in the myocardium over the cardiac cycle. If the movement in a single point was strictly one directional and uniform during the cardiac cycle, the vector loops in Fig. 8 should have been a straight line in all three 2D planes. Our findings show that regional myocardial motion is truly a three-directional movement, and caution should be taken when assessing myocardial function using either a 1D or 2D imaging technique. Since our method allows us to study any region of the left ventricle after acquisition, we are not constrained to study wall motion abnormalities that may not have been known at the time of the actual acquisition.

Strain rate, as a parameter to assess local expansion and compression, has been used within the cardiac ultrasound community as a complement to DMI (Heimdahl et al., 1998). The 3D velocity data acquired from our measurements can be studied directly, or used for calculations of strain rate or

strain, without the angle sensitivity that is a problem using Doppler data (Arai et al., 1999). A better understanding of normal physiological and pathophysiological responses of the myocardium in three dimensions could improve our knowledge and interpretation of the heart in situ as a truly 3D organ. Our method opens up a possibility to assess three-directional myocardial strain rate and strain in healthy volunteers and in any patient group.

### Study Limitations

A drawback of our technique is the low temporal resolution, resulting in an underestimation of the peak systolic and diastolic velocity values. The 3D PC-MRI technique will, however, provide data describing all three velocity components and hence the direction of the motion in 3D space. The long acquisition time makes our tool foremost applicable to basal understanding of cardiac function, and is not ready for clinical use yet. Further refinement of the acquisition scheme with the use of parallel imaging and other recent scanner technologies could reduce the scan time as well as improve the temporal resolution. The time needed for postprocessing of the velocity data is less than 1 hour. The analysis includes the positioning of a cursor in the 3D space to extract the velocity data from the points of interest. Consequently, the number of points will also determine the time needed for the analysis. Our data has not been compensated for any interference secondary to the respiratory motion, which degrades the quality of the data by introducing a slight blurring. The points from which we extract our data are fixed over time. As the heart moves, the point will move through the whole wall and generate data from both subendocardial and subepicardial layers.

### CONCLUSIONS

The time-resolved 3D phase contrast MRI technique makes it feasible to extract myocardial velocities for all three velocity components and describe the motion of the left ventricle without the need for placing any slices at the time for the acquisition.

### ACKNOWLEDGMENTS

This work was supported by the Swedish Heart and Lung Foundation, the Swedish Research Council (grant no. 09481), and the County Council of Östergötland, Sweden. This work was presented in part



at the ESMRMB 17th annual meeting in Paris, France, September 14–17, 2000.

### REFERENCES

- Aletras, A. H., Balaban, R. S., Wen, H. (1999). High-resolution strain analysis of the human heart with fast-DENSE. *J. Magn. Reson.* 140:41–57.
- Arai, A. E., Gaither, C. C. 3rd, Epstein, F. H., Balaban, R. S., Wolff, S. D. (1999). Myocardial velocity gradient imaging by phase contrast MRI with application to regional function in myocardial ischemia. *Magn. Reson. Med.* 42:98–109.
- Axel, L., Dougherty, L. (1989). MR imaging of motion with spatial modulation of magnetization. *Radiology* 171:841–845.
- Bernstein, M. A., Zhou, X. J., Polzin, J. A., King, K. F., Ganin, A., Pelc, N. J., Glover, G. H. (1998). Concomitant gradient terms in phase contrast MR: analysis and correction. *Magn. Reson. Med.* 39:300–308.
- Bogaert, J., Rademakers, F. E. (2001). Regional nonuniformity of normal adult human left ventricle. *Am. J. Physiol. Heart Circ. Physiol.* 280: H610–H620.
- DeGroot, C. (2003). Doppler strain rate echocardiography versus magnetic resonance imaging. *Circulation* 107:e23, author reply e23.
- Drangova, M., Zhu, Y., Pelc, N. J. (1997). Effect of artifacts due to flowing blood on the reproducibility of phase-contrast measurements of myocardial motion. *J. Magn. Reson. Imaging* 7:664–668.
- Ebbers, T., Wigström, L., Bolger, A. F., Wranne, B., Karlsson, M. (2002). Noninvasive measurement of time-varying three-dimensional relative pressure fields within the human heart. *J. Biomech. Eng.* 124:288–293.
- Fleming, A. D., Xia, X., McDicken, W. N., Sutherland, G. R., Fenn, L. (1994). Myocardial velocity gradients detected by Doppler imaging. *Br. J. Radiol.* 67:679–688.
- Gorcsan, J. 3rd, Gulati, V. K., Mandarino, W. A., Katz, W. E. (1996). Color-coded measures of myocardial velocity throughout the cardiac cycle by tissue Doppler imaging to quantify regional left ventricular function. *Am. Heart J.* 131:1203–1213.
- Hansen, D. E., Daughters, G. T. 2nd, Alderman, E. L., Ingels, N. B. Jr., Miller, D. C. (1988). Torsional deformation of the left ventricular midwall in human hearts with intramyocardial markers: regional heterogeneity and sensitivity to the inotropic effects of abrupt rate changes. *Circ. Res.* 62:941–952.
- Hatle, L., Sutherland, G. R. (2000). Regional myocardial function—a new approach. *Eur. Heart J.* 21:1337–1357.
- Heimdal, A., Stoylen, A., Torp, H., Skjaerpe, T. (1998). Real-time strain rate imaging of the left ventricle by ultrasound. *J. Am. Soc. Echocardiogr.* 11:1013–1019.
- Herzka, D. A., Guttman, M. A., McVeigh, E. R. (2003). Myocardial tagging with SSFP. *Magn. Reson. Med.* 49:329–340.
- Holman, E. R., Buller, V. G., de Roos, A., van der Geest, R. J., Baur, L. H., van der Laarse, A., Bruschke, A. V., Reiber, J. H., van der Wall, E. E. (1997). Detection and quantification of dysfunctional myocardium by magnetic resonance imaging. A new three-dimensional method for quantitative wall-thickening analysis. *Circulation* 95:924–931.
- Ingels, N. B. Jr., Hansen, D. E., Daughters, G. T. 2nd, Stinson, E. B., Alderman, E. L., Miller, D. C. (1989). Relation between longitudinal, circumferential, and oblique shortening and torsional deformation in the left ventricle of the transplanted human heart. *Circ. Res.* 64:915–927.
- Jones, C. J., Raposo, L., Gibson, D. G. (1990). Functional importance of the long axis dynamics of the human left ventricle. *Br. Heart J.* 63:215–220.
- Karwatowski, S. P., Mohiaddin, R., Yang, G. Z., Firmin, D. N., Sutton, M. S., Underwood, S. R., Longmore, D. B. (1994). Assessment of regional left ventricular long-axis motion with MR velocity mapping in healthy subjects. *J. Magn. Reson. Imaging* 4:151–155.
- Kaysers, H. W., van der Geest, R. J., van der Wall, E. E., Duchateau, C., de Roos, A. (2000). Right ventricular function in patients after acute myocardial infarction assessed with phase contrast MR velocity mapping encoded in three directions. *J. Magn. Reson. Imaging* 11:471–475.
- Madore, B., Fredrickson, J. O., Alley, M. T., Pelc, N. J. (2000). A reduced field-of-view method to increase temporal resolution or reduce scan time in cine MRI. *Magn. Reson. Med.* 43:549–558.
- Masood, S., Yang, G. Z., Pennell, D. J., Firmin, D. N. (2000). Investigating intrinsic myocardial mechanics: the role of MR tagging, velocity phase mapping, and diffusion imaging. *J. Magn. Reson. Imaging* 12:873–883.
- Miyatake, K., Yamagishi, M., Tanaka, N., Uematsu, M., Yamazaki, N., Mine, Y., Sano, A., Hiram, M. (1995). New method for evaluating left ventricular



- wall motion by color-coded tissue Doppler imaging: in vitro and in vivo studies. *J. Am. Coll. Cardiol.* 25:717–724.
- Osman, N. F., Kerwin, W. S., McVeigh, E. R., Prince, J. L. (1999). Cardiac motion tracking using CINE harmonic phase (HARP) magnetic resonance imaging. *Magn. Reson. Med.* 42:1048–1060.
- Pelc, L. R., Sayre, J., Yun, K., Castro, L. J., Herfkens, R. J., Miller, D. C., Pelc, N. J. (1994). Evaluation of myocardial motion tracking with cine-phase contrast magnetic resonance imaging. *Invest. Radiol.* 29:1038–1042.
- Popp, R. L. (1990). Echocardiography (2). *N. Engl. J. Med.* 323:165–172.
- Ryf, S., Spiegel, M. A., Gerber, M., Boesiger, P. (2002). Myocardial tagging with 3D-CSPAMM. *J. Magn. Reson. Imaging* 16:320–325.
- Sampath, S., Derbyshire, J. A., Atalar, E., Osman, N. F., Prince, J. L. (2003). Real-time imaging of two-dimensional cardiac strain using a harmonic phase magnetic resonance imaging (HARP-MRI) pulse sequence. *Magn. Reson. Med.* 50:154–163.
- Sutherland, G. R., Stewart, M. J., Groundstroem, K. W., Moran, C. M., Fleming, A., Guell-Peris, F. J., Riemersma, R. A., Fenn, L. N., Fox, K. A., McDicken, W. N. (1994). Color Doppler myocardial imaging: a new technique for the assessment of myocardial function. *J. Am. Soc. Echocardiogr.* 7:441–458.
- Uematsu, M., Miyatake, K., Tanaka, N., Matsuda, H., Sano, A., Yamazaki, N., Hiramata, M., Yamagishi, M. (1995). Myocardial velocity gradient as a new indicator of regional left ventricular contraction: detection by a two-dimensional tissue Doppler imaging technique. *J. Am. Coll. Cardiol.* 26:217–223.
- Wigström, L., Sjöqvist, L., Wranne, B. (1996). Temporally resolved 3D phase-contrast imaging. *Magn. Reson. Med.* 36:800–803.
- Wigström, L., Ebbers, T., Fyrenius, A., Karlsson, M., Engvall, J., Wranne, B., Bolger, A. F. (1999). Particle trace visualization of intracardiac flow using time-resolved 3D phase contrast MRI. *Magn. Reson. Med.* 41:793–799.
- Wranne, B., Pinto, F. J., Hammarstrom, E., St Goar, F. G., Puryear, J., Popp, R. L. (1991). Abnormal right heart filling after cardiac surgery: time course and mechanisms. *Br. Heart J.* 66:435–442.
- Wranne, B., Pinto, F. J., Siegel, L. C., Miller, D. C., Schnittger, I. (1993). Abnormal postoperative interventricular motion: new intraoperative transesophagealechocardiographic evidence supports a novel hypothesis. *Am. Heart J.* 126:161–167.
- Zerhouni, E. A., Parish, D. M., Rogers, W. J., Yang, A., Shapiro, E. P. (1988). Human heart: tagging with MR imaging—a method for noninvasive assessment of myocardial motion. *Radiology* 169:59–63.
- Zwanenburg, J. J., Kuijper, J. P., Marcus, J. T., Heethaar, R. M. (2003). Steady-state free precession with myocardial tagging: CSPAMM in a single breath-hold. *Magn. Reson. Med.* 49:722–730.



## **Request Permission or Order Reprints Instantly!**

Interested in copying and sharing this article? In most cases, U.S. Copyright Law requires that you get permission from the article's rightsholder before using copyrighted content.

All information and materials found in this article, including but not limited to text, trademarks, patents, logos, graphics and images (the "Materials"), are the copyrighted works and other forms of intellectual property of Marcel Dekker, Inc., or its licensors. All rights not expressly granted are reserved.

Get permission to lawfully reproduce and distribute the Materials or order reprints quickly and painlessly. Simply click on the "Request Permission/Order Reprints" link below and follow the instructions. Visit the [U.S. Copyright Office](#) for information on Fair Use limitations of U.S. copyright law. Please refer to The Association of American Publishers' (AAP) website for guidelines on [Fair Use in the Classroom](#).

The Materials are for your personal use only and cannot be reformatted, reposted, resold or distributed by electronic means or otherwise without permission from Marcel Dekker, Inc. Marcel Dekker, Inc. grants you the limited right to display the Materials only on your personal computer or personal wireless device, and to copy and download single copies of such Materials provided that any copyright, trademark or other notice appearing on such Materials is also retained by, displayed, copied or downloaded as part of the Materials and is not removed or obscured, and provided you do not edit, modify, alter or enhance the Materials. Please refer to our [Website User Agreement](#) for more details.

### **[Request Permission/Order Reprints](#)**

Reprints of this article can also be ordered at

<http://www.dekker.com/servlet/product/DOI/101081JCMR120038692>